GEOPHYSICAL RESEARCH LETTERS, VOL. 40, 1–6, doi:10.1002/grl.50698, 2013

Determining the orientations of ocean bottom seismometers using ambient noise correlation

Yang Zha,[1] Spahr C. Webb,[1] and William Menke[1]

Received 25 April 2013; revised 16 June 2013; accepted 24 June 2013.

[1] The cross-correlation of multicomponent ambient seismic noise can reveal both the velocity and polarization of surface waves propagating between pairs of stations. We explore this property to develop a novel method for determining the horizontal orientation of ocean bottom seismometers (OBS) by analyzing the polarization of Rayleigh waves retrieved from ambient noise cross-correlation. We demonstrate that the sensor orientations can be estimated through maximizing the correlation between the radial-vertical component and the phase-shifted vertical-vertical component of the empirical Green's tensor. We apply this new method to the ELSC (Eastern Lau Spreading Center) OBS experiment data set and illustrate its robustness by comparing the obtained orientations with results from a conventional method utilizing teleseismic *P* and Rayleigh wave polarizations. When applied to a large OBS array, the ambient noise method provides a larger number of orientation estimates and better azimuthal coverage than typically is possible with traditional methods. **Citation:** Zha, Y., S. C. Webb, and W. Menke (2013), Determining the orientations of ocean bottom seismometers using ambient noise correlation, *Geophys. Res. Lett.*, *40*, doi:10.1002/grl.50698.

1. Introduction

[2] Ocean bottom seismometer (OBS) arrays have become powerful tools for studying the structure and dynamics of the oceanic crust and mantle. During typical OBS deployments, sensors are settled onto the seafloor through a free-fall process, leading to unknown horizontal orientation of the OBS sensors. Well-orientated horizontal component data are critical to the analysis of anisotropy, receiver functions, and surface wave dispersion. To determine sensor orientations, some deployments have used air gun shots from known locations [*Anderson et al.*, 1987; *Duennebier et al.*, 1987], but these active sources are not available in many passive OBS experiments. Teleseismic methods for obtaining sensor orientations include analyzing the polarization of *P* wave or Rayleigh wave from known earthquakes [*Stachnik et al.*, 2012] and calculating the correlation between data and synthetic seismograms [*Ekström and Busby*, 2008]. However, the noise levels on the horizontal channels of OBS are usually high in teleseismic frequency bands (20–100 s period) due to ocean bottom currents and infragravity waves [*Crawford and Webb*, 2000], limiting the number of high-quality teleseismic events utilized. Moreover, when the majority of teleseismic events used come from a small range of back azimuths, inferred sensor orientations can be biased by ray bending effects due to velocity heterogeneity outside of the array [*Laske*, 1995].

[3] Cross-correlation of ambient seismic noise records can be used to infer the impulse response function (or "Green's tensor") between pairs of stations; that is, the seismic signal that would be observed at one station due to a force applied at the other [*Bensen et al.*, 2007; *Shapiro*, 2004; *Snieder*, 2004]. In ambient noise tomography, vertical component seismograms are commonly cross-correlated to infer the vertical response at one station due to a vertical force at the other. The phase velocities of Rayleigh waves propagating between station pairs are measured and used in tomographic inversions for subsurface velocity structure [*Ekström et al.*, 2009; *Lin et al.*, 2008; *Shapiro et al.*, 2005]. We discuss here another complimentary use. The cross-correlation between the vertical and radial components yield the "cross terms" of the Green's tensor [*van Wijk et al.*, 2011], which represent the radial signal observed at one station due to a vertical force at the other:

$$G_{rz}(x,x',t) + G_{rz}(x,x',-t) \propto \langle U_r(x,t) \star U_z(x',t) \rangle \quad (1)$$

Here $G_{rz}(x,x',t)$ is the radial component Green's tensor at x due to a vertical point source at x', $U_r(x,t)$ and $U_z(x',t)$ stand for radial and vertical displacements at x and x', respectively. $\star$ denotes cross-correlation, and $\langle\rangle$ denotes ensemble average by temporal stacking.

[4] The Rayleigh wave part of the impulse response is elliptically polarized in the vertical-radial plane, so the radial motion is phase-shifted 90° with respect to the vertical. In the frequency domain

$$G_{rz}(x,x',\omega) \propto G_{zz}(x,x',\omega)e^{-i\pi/2} \quad (2)$$

Here we present a method to estimate the optimal sensor orientations by finding the orientation azimuth that maximizes the correlation between the measured response functions G_{rz} and G_{zz} between station pairs. Because the interstation ray paths are usually shorter than teleseismic ray paths and often have better azimuthal coverage as well, the orientations determined using this method should be less biased by ray bending effects than are teleseismic methods. Furthermore, since the number of orientation estimates for a given station increases with the number of stations in the array, this method should be more accurate for OBS arrays with large numbers of stations. We apply this method to the ELSC OBS array data collected at the Eastern Lau Spreading Center and compare these orientation results with results from a conventional method utilizing teleseismic *P* and Rayleigh waves.

Additional supporting information may be found in the online version of this article.

[1]Lamont-Doherty Earth Observatory, Columbia University, Palisades, New York, USA.

Corresponding author: Y. Zha, Lamont-Doherty Earth Observatory, Columbia University, Palisades 10964, NY, USA. (yangz@ldeo.columbia.edu)

0094-8276/13/10.1002/grl.50698

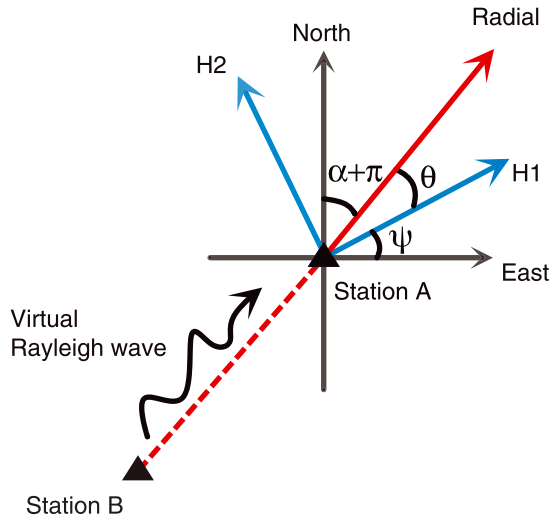

Figure 1. Illustration of the coordinate systems and virtual Rayleigh wave propagating from station B to A used to calculate orientation angle for A. H_1 and H_2: orthogonal OBS components of unknown direction; ψ : orientation angle for A; α: back azimuth from A to B; θ: correction angle to rotate H_1 and H_2 component to radial and transverse direction.

We also discuss data selection procedures that will improve the quality of orientation estimates.

2. Ambient Noise Orientation Method

[5] The algorithm for obtaining sensor orientations consists of three major steps. (1) Calculating the three-component Green's functions for all station pairs by noise cross-correlation, (2) measurement of sensor orientation through an optimization process, and (3) data selection and statistical analysis to obtain final orientation angles.

[6] The raw OBS data are provided in one vertical component (Z) and two orthogonal horizontal components (H_1 and H_2) of unknown directions. The orientation angle ψ for one station is defined here as the angle counter-clockwise from east to H_1 (Figure 1). For each station whose orientation angle is to be determined (denoted as station A), we estimate its three-component impulse response functions due to a point vertical force at another station (denoted as station B) by calculating and stacking the daily cross-correlation functions (CCFs) between each of the three-component signals at A and the vertical component signal at B:

$$C_{iz}(t) = \langle U_i^A(t) \star U_z^B(t) \rangle; i = 1, 2, z; \quad (3)$$

where C_{iz} is the stacked CCF between the ith component of station A and the vertical component at station B. To preserve the relative amplitude between the two horizontal impulse response functions for the later rotation process, data are not clipped by the commonly used one-bit normalization before cross-correlation. Instead, the daily CCFs are normalized prior to stacking to ensure that the stacked CCFs are not dominated by a few large earthquakes [*Bensen et al.*, 2007]. The two cross terms of CCF C_{1z} and C_{2z} are normalized together to preserve particle motion information. To reduce the effect of non-uniform source distribution, we fold the positive and negative lag of the CCF to obtain the symmetric cross-correlation signal [*Bensen et al.*, 2007].

The symmetric CCFs are then filtered to the frequency band where strongest Rayleigh wave are expected to emerge. For OBS in deep ocean (>1000 m), the main noise sources that contribute to the emergence of Rayleigh waves are in the microseism band (0.05–0.2 Hz) [*Yang and Ritzwoller*, 2008; *Webb*, 1998].

[7] We then estimate the angle θ needed to rotate the $H_1 - H_2$ coordinate system into radial-transverse coordinate, using the guiding principle that the true θ will maximizes the zero-lag cross-correlation between the radial response function C_{rz} and phase-shifted vertical response function $\tilde{C}_{zz}$. The 90° phase shift is computed using Hilbert transform, following *Baker* [2004]. The optimization is performed via a grid search with 1° steps. θ depends on both the seismometer

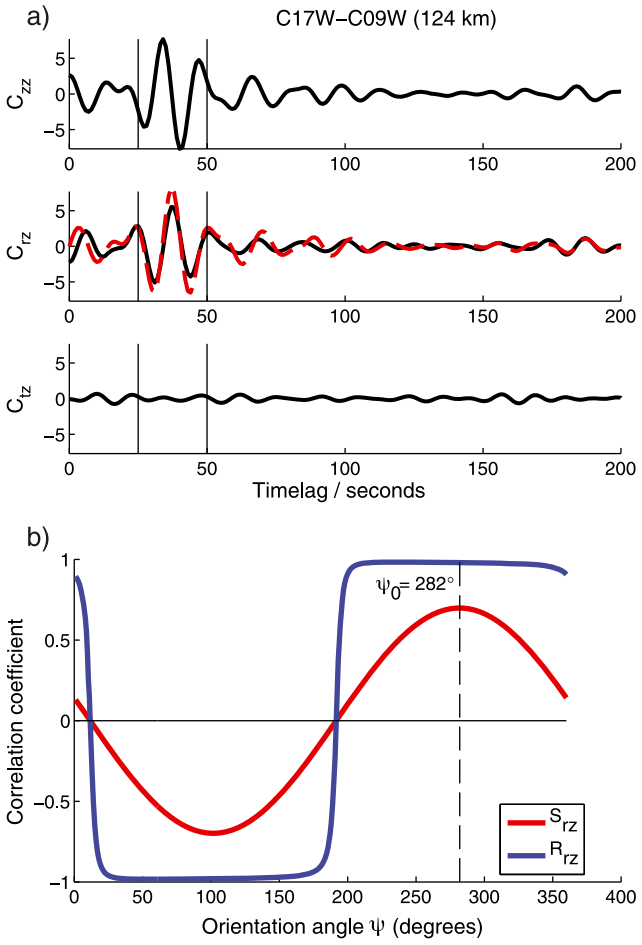

Figure 2. (a) Three-component Rayleigh wave impulse response functions estimated from cross-correlation between station pair C17W-C09W and rotated to a vertical-radial-transverse coordinate system. Top to bottom: C_{zz}, C_{rz}, and C_{tz} are shown in black; dashed red line in middle panel represents $\tilde{C}_{zz}$, 90° phase-shifted C_{zz}; vertical thin black lines indicate time window corresponding to group velocity of 2.5–5 km/s used to calculate correlation coefficient. (b) Correlation between C_{rz} and $\tilde{C}_{zz}$ as a function of possible orientation angle ψ. Red: correlation coefficient S_{rz} defined in equation (5) used to determine the orientation angle; blue: normalized correlation coefficient R_{rz} (equation (6)) used for quality control; vertical dashed line marks the measured orientation at which S_{rz} is a maximum.

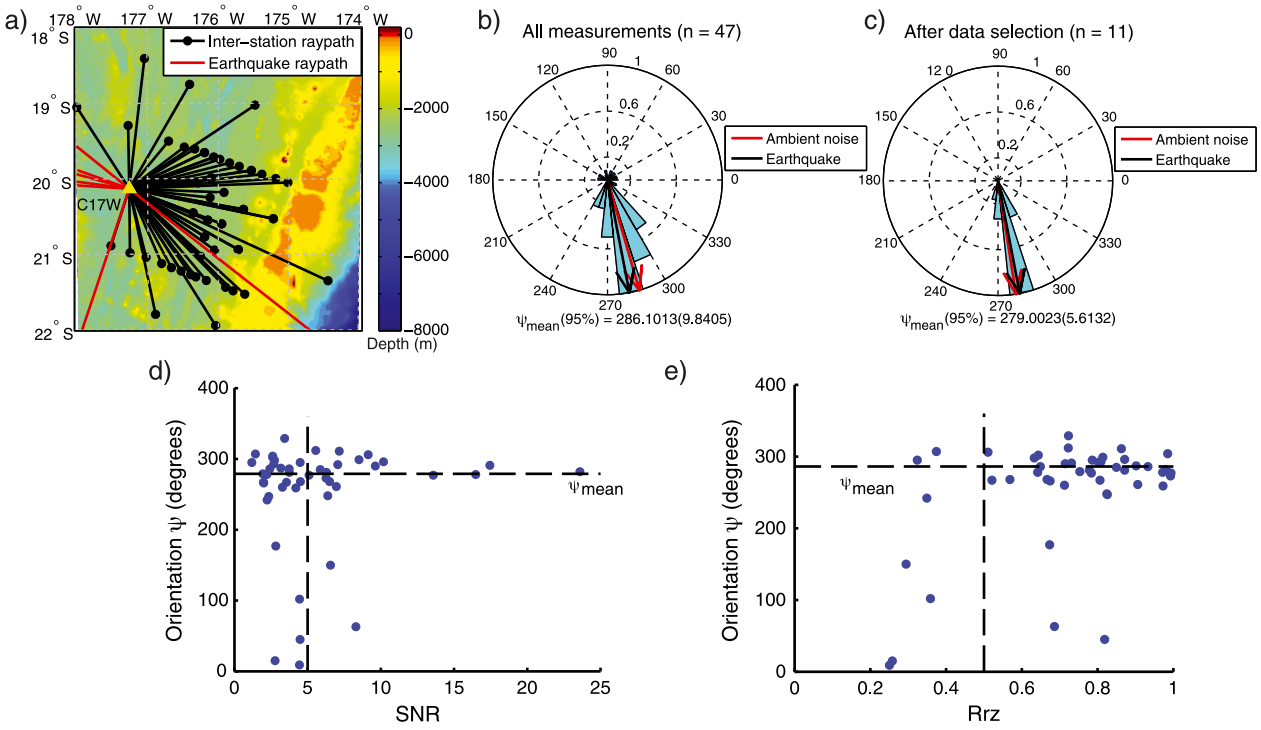

Figure 3. (a) ELSC OBS array map and ray path coverage for orienting OBS C17W; black lines: interstation ray paths; red lines: event-station great circle ray paths used by teleseismic method; solid triangle: OBS C17W; solid black dots: OBS used to calculate ambient noise correlation with C17W. Background color represent seafloor bathymetry. (b) Normalized polar distribution of all orientation measurements from 47 station pairs; Red arrow marks the mean of determined sensor orientation using ambient noise method; Black arrow marks the mean orientation determined from teleseismic waveforms; value of the mean orientation angle ψ_{mean} and 95% confidence interval (in parenthesis) are also shown. (c) Same as Figure 3b, but after data selection. (d) Orientation measurements as a function of signal to noise ratio (SNR) of C_{rz} between each station pair.(e) Orientation measurements as a function of R_{rz}, the coherence between C_{rz} and $\tilde{C}_{zz}$ (equation (6)). In Figures 3d and 3e, horizontal dashed line marks the mean orientation angle shown in Figures 3c; vertical dashed line marks the cutoff value used.

orientation angle ψ and the back azimuth α_{AB} from station A to B through $\theta = \frac{\pi}{2} - (\alpha_{AB} + \pi) - \psi$ (Figure 1). Back azimuth is computed from the known station coordinates using spherical geometry. To rotate C_{1z} and C_{2z} to the radial and transverse components C_{rz}, C_{tz}:

$$\begin{pmatrix} C_{rz} \\ C_{tz} \end{pmatrix} = \begin{pmatrix} \cos\theta & \sin\theta \\ -\sin\theta & \cos\theta \end{pmatrix} \begin{pmatrix} C_{1z} \\ C_{2z} \end{pmatrix} \tag{4}$$

The cross-correlation and rotation operations commute, therefore, results do not depend upon the order in which they are performed [*Lin et al.*, 2008]. However, performing the cross-correlation prior to rotation significantly reduces the computation cost.

[8] The least-squares estimate of the linear correlation coefficient $S_{rz}(\psi)$ between C_{rz} and $\tilde{C}_{zz}$ is calculated as (following *Stachnik et al.* [2012] and *Baker* [2004]):

$$S_{rz}(\psi) = \frac{\rho(C_{rz}, \tilde{C}_{zz})}{\rho(\tilde{C}_{zz}, \tilde{C}_{zz})} \tag{5}$$

in which $\rho(X, Y) = \int_{t_1}^{t_2} X(t)Y(t)\mathrm{d}t$ is the zero-lag cross-correlation between two time series X and Y, and $[t_1, t_2]$ is the time window of Rayleigh wave arrival calculated based on specified range of group velocities. $\rho(C_{rz}, \tilde{C}_{zz})$ is a function of ψ, whereas $\rho(\tilde{C}_{zz}, \tilde{C}_{zz})$ is just a normalization factor.

Figure 2 illustrates the process of estimating the orientation for station C17W using cross-correlation between the OBS pair C17W-C09W. High correlation between C_{rz} and $\tilde{C}_{zz}$ suggests successful retrieval of Rayleigh wave from the ambient noise cross-correlation (Figure 2a).

[9] We perform the above analysis for all station pairs containing the target station A to obtain a series of independent measurements of the orientation angle. As an example, orientation results for OBS C17W are shown in Figure 3. The large number of available interstation ray paths lead to an excellent azimuthal coverage (Figure 3a). The mean orientation from the ambient noise method is approximately equal to the orientation determined from polarization analysis of teleseismic Rayleigh waves (with a deviation of 1.92°) (Figures 3b and 3c). Several factors may introduce errors and variability to the measurements, such as nonuniform distribution of ambient noise source, instrument noise, and various propagation effects including anisotropy, scattering, and off-great circle ray paths. Careful quality control procedures are thus needed to filter out low-quality measurements and to obtain an accurate orientation angle. We apply the following criteria to refine the measurements:

[10] 1. Signal to noise ratio (SNR) of the Rayleigh wave impulse responses function: to ensure the emergence of Rayleigh wave on the radial-vertical cross-correlation function C_{rz}, we measure the SNR of C_{rz} as the ratio of the peak

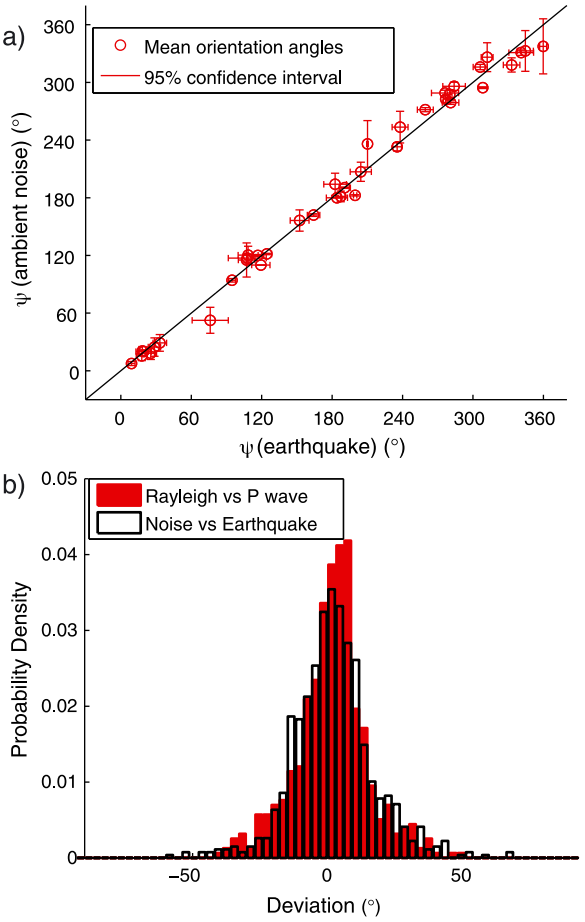

Figure 4. (a) Comparison of orientation angles determined by teleseismic method (horizontal axis) and the ambient noise method (vertical axis), thin black line marks $x = y$. Values presented here are mean orientation angles and their 95% confidence intervals after data selection (see text for details).(b) Open bars: distribution of the deviation between orientation measurements from the ambient noise method and teleseismic method ($\sigma = 14.3°$). Deviations are calculated from all possible pairs of measurements for each station, stacked over all stations, binned into 3° intervals and normalized by the number of pairs. Distribution of the deviations between Rayleigh wave and P wave measurements from teleseismic events ($\sigma = 13.5°$, filled bars) are shown as comparison.

amplitude within Rayleigh wave window to the rms average of the tailing noise [*Bensen et al.*, 2007]. The SNR of C_{rz} is generally lower than SNR of C_{zz} due to the high noise level on the horizontal OBS channels. Variability of calculated orientation angles becomes quite high when SNR < 5. (Figure 3d). To exclude unreliable measurements, we only use measurement with both SNR >= 5.

[11] 2. The coherence between C_{rz} and $\tilde{C}_{zz}$: We use the normalized correlation coefficient R_{rz},

$$R_{rz}(\psi) = \frac{\rho(C_{rz}, \tilde{C}_{zz})}{\sqrt{\rho(C_{rz}, C_{rz})\rho(\tilde{C}_{zz}, \tilde{C}_{zz})}} \quad (6)$$

because it has a well-defined range of [–1, 1] [*Baker*, 2004], in contrast to $S_{rz}(\psi)$, which is unbounded. Empirically, measurements with $R_{rz} > 0.5$ are much less scattered than those with $R_{rz} < 0.5$ (Figure 3e), similar to that observed by *Stachnik et al.* [2012] using teleseismic Rayleigh waves.

[12] After the data selection process, the remaining measurements show a much smaller scatter (Figure 3c). The mean orientation angles $\bar{\psi}$ and their uncertainties can be obtained through circular statistical analysis of the refined data set [*Berens*, 2009].

3. Application to ELSC OBS Array

[13] We apply the ambient noise orientation method to 51 three-component broadband OBSs deployed during the ELSC experiment at the Eastern Lau Spreading Center from November 2009 to November 2010. Daily OBS data are first corrected for clock drift, then three-component symmetric cross-correlation functions (CCFs) are calculated and stacked for all station pairs at distances larger than 80 km. All CCFs are filtered to 0.05–0.1 Hz and cut to time windows corresponding to group velocities of 2.5–5 km/s. For each station, a series of polarization measurements are made using the automated algorithm. This preliminary data set is then refined by applying the two selection criteria described in section 2. There is a trade-off between the minimum accepted value of SNR and the number of qualified measurements. In order to exclude low-quality measurements while keeping a sizable data set, we use the following cutoff values: $R_{rz} > 0.5$ and $SNR > 5$. We then use a bootstrap algorithm to estimate the uncertainties of the mean orientation angles [*Menke and Menke*, 2009], and keep only measurements within the 95% confidence interval [*Stachnik et al.*, 2012]. This process will likely reduce bias introduced by outliers. The final estimate of the orientation angle is then calculated as the circular mean of the refined measurements.

[14] To evaluate the robustness of the ambient noise orientation method, we compare the obtained orientation angles to results from the conventional method utilizing teleseismic earthquakes for the ELSC stations (Figure 4, for detail, see supporting information, Table S1). The conventional method uses P and Rayleigh wave arrivals from eight Mw≥ 7.0 events that occurred during the array deployment. This small number of usable teleseismic events is due to the high level of horizontal noise and local seismicity near the OBS array. Orientation angles are independently determined either by maximizing the zero-lag cross-correlation between vertical and radial signals for the P wave arrival, or between the radial and phase-shifted vertical signal for the Rayleigh wave arrival. Measurements are accepted only when the orientation obtained from P wave and Rayleigh wave for the same event agree within 10°. As shown in Figure 4a, the orientation angles determined using the conventional method and the ambient noise method show good agreement, with a rms deviation of 9.6° and a correlation coefficient of 0.995. The consistency between these two methods indicates that the ambient noise method is providing robust and accurate orientation measurements.

4. Discussion

[15] A unique property of the ambient noise orientation method is the increasing number of virtual Rayleigh wave sources with the number of OBS sites, which makes this technique even more effective for OBS arrays with a large number of stations (which are becoming increasingly

common). In contrast, the number of usable teleseismic signals is limited by the length of the deployment, especially for "noisy" regions near major tectonic boundaries. Another potential advantage is that the sites will often have denser and wider azimuthal interstation path coverage than teleseismic arrivals (Figure 3a), which often come from a few directions corresponding to tectonically active regions (e.g., nearby subduction zones). Because both the causal and acausal parts of the CCFs are used, the stacked symmetric CCF contains information of waves traveling in both directions along an interstation path. Therefore, the actual azimuth coverage may be twice the apparent coverage. Such wide azimuthal coverage may reduce biases introduced by propagation effects such as off-great circle ray paths due to velocity anomalies and out-of-plane Rayleigh wave motion caused by local anisotropy [*Stachnik et al.*, 2012; *Ekström and Busby*, 2008], leading to more accurate orientation measurements. Some outer stations have less azimuthal coverage compared to the center stations and may be more affected by ray bending and anisotropy. An approach to further reduce these effects may be to first obtain Rayleigh wave phase velocity and anisotropy map within the array from ambient noise tomography using vertical CCFs, then forward model to the arrival angles and polarizations for each station pair to include in calculating orientations.

[16] As with methods using ambient noise cross-correlation to estimate surface wave velocities, the ambient noise orientation method relies on the commonly adopted assumption of an isotropic stochastic wavefield [*Ekström et al.*, 2009; *Harmon et al.*, 2010]. Nonuniform noise sources could introduce errors into the estimates of orientation angle. However, studies have shown that except for a few locations [*Shapiro et al.*, 2006], the azimuthal distribution of ambient noise sources are generally smooth [*Harmon et al.*, 2010], in which case the time averaged empirical Green's functions is similar to that from an isotropic noise distribution [*Lin et al.*, 2008]. The consistency between orientation angles obtained from this method and the teleseismic method indicates that no significant systematic errors are introduced in this example by the isotropic wavefield assumption. The effects of nonuniform noise distribution on the obtained orientation will be the subject of future investigations.

[17] Seafloor topography, local currents, and other uncorrelated noises may introduce bias and errors into the orientation measurements. In Figure 4b, we show that distribution of differences between individual measurements from the ambient noise method and from the teleseismic method are quite similar to that of the differences between *P* and Rayleigh wave measurements within the teleseismic measurements. This suggests that the inconsistency between results from the two orientation method is not significantly higher than the inconsistency within the teleseismic data sets. Therefore, we believe that the ambient noise method is not subject to a higher level of errors and bias introduced by these factors than the teleseismic method.

[18] The orientation method presented in this study exploits the elliptical Rayleigh wave motion by analyzing C_{rz}, the cross term of the empirical Green's function, and its correlation with the diagonal term C_{zz}. This scheme is straightforward as it tries to determine the orientation of one station at a time. A possible alternative scheme is to evaluate the C_{rr} term and its correlation with C_{zz}. While such scheme does not involve calculating cross terms, C_{1z} and C_{2z}, it requires grid searching over both stations' orientations and is more computation intensive. Comparing the robustness of these two schemes will be addressed in future studies. It may also be practical to use C_{rr} correlations between OBS and well-oriented land stations to obtain orientations. Finally, we note that it should be possible to conduct a similar orientation analysis in the frequency domain, using coherence instead of cross-correlation as the measure of waveform similarity.

5. Conclusion

[19] We have developed a new method for obtaining reliable OBS orientations through polarization analysis of virtual Rayleigh waves retrieved from ambient noise cross-correlation. We demonstrate that the horizontal orientation of OBS sensors can be estimated by maximizing the correlation between the C_{rz} and C_{zz} terms of the response functions (Green's tensor). The data quantity and azimuthal coverage of ray paths for the ambient noise method increase with the number of sensors, making it potentially more accurate for large OBS arrays. Orientation results of ELSC OBS array are highly consistent with results from conventional earthquake-based method, indicating that the ambient noise method is providing robust orientation measurements. Capable of measuring orientations continuously and during short-term deployments, the new technique will allow more accurate retrieval of horizontal OBS signals. Furthermore, its application can be extended to verifying land seismometer orientations and obtaining borehole seismometer orientations

[20] **Acknowledgments.** We thank the scientific party, captain, crew, and technical team of R/V *Kilo Moana* and R/V *Roger Revelle* for their work that made this study possible. We thank Douglas Wiens, Donna Blackman, Robert Dunn, and James Conder for careful cruise planning and the OBS teams of both cruises for their tireless help in deploying and recovering the instruments as well as providing sensor response information. Y. Zha thanks Göran Ekström, Ge Jin, and Zach Eilon for their inspiring discussions. This work was supported by a National Science Foundation grant: OCE04-26369.

[21] The Editor thanks Douglas Wiens and an anonymous reviewer for their assistance in evaluating this paper.

References

Anderson, P. N., F. K. Duennebier, and R. K. Cessaro (1987), Ocean borehole horizontal seismic sensor orientation determined from explosive charges, *J. Geophys. Res. Solid Earth*, *92*(B5), 3573–3579.

Baker, G. E. (2004), Backazimuth estimation reliability using surface wave polarization, *Geophys. Res. Lett.*, *31*, L09611, doi:10.1029/2004GL019510.

Bensen, G. D., M. H. Ritzwoller, M. P. Barmin, A. L. Levshin, F. Lin, M. P. Moschetti, N. M. Shapiro, and Y. Yang (2007), Processing seismic ambient noise data to obtain reliable broad-band surface wave dispersion measurements, *Geophys. J. Int.*, *169*(3), 1239–1260, doi:10.1111/j.1365-246X.2007.03374.x.

Berens, P. (2009), CircStat: A MATLAB toolbox for circular statistics, *J. Stat. Softw.*, *31*(10), 1–21.

Crawford, W., and S. Webb (2000), Identifying and removing tilt noise from low-frequency (<0.1 Hz) seafloor vertical seismic data, *Bull. Seismol. Soc. Am.*, *90*(4), 952–963.

Duennebier, F. K., P. N. Anderson, and G. J. Fryer (1987), Azimuth determination of and from horizontal ocean bottom seismic sensors, *J. Geophys. Res.*, *92*(B5), 3567–3572.

Ekström, G., and R. W. Busby (2008), Measurements of seismometer orientation at USArray Transportable Array and Backbone stations, *Seismol. Res. Lett.*, *79*(4), 554–561, doi:10.1785/gssrl.79.4.554.

Ekström, G., G. A. Abers, and S. C. Webb (2009), Determination of surface-wave phase velocities across USArray from noise and Aki's spectral formulation, *Geophys. Res. Lett.*, *36*(18), L18301, doi:10.1029/2009GL039131.

Harmon, N., C. Rychert, and P. Gerstoft (2010), Distribution of noise sources for seismic interferometry, *Geophys. J. Int.*, *183*(3), 1470–1484, doi:10.1111/j.1365-246X.2010.04802.x.

Laske, G. (1995), Global observation of off-great-circle propagation of long-period surface waves, *Geophys. J. Int.*, *123*(1), 245–259.

Lin, F.-C., M. P. Moschetti, and M. H. Ritzwoller (2008), Surface wave tomography of the western United States from ambient seismic noise: Rayleigh and Love wave phase velocity maps, *Geophys. J. Int.*, *173*(1), 281–298, doi:10.1111/j.1365-246X.2008.03720.x.

Menke, W., and J. Menke (2009), *Environmental Data Analysis with MATLAB*, 288 pp., Elsevier, New York.

Shapiro, N. M. (2004), Emergence of broadband Rayleigh waves from correlations of the ambient seismic noise, *Geophys. Res. Lett.*, *31*, L07614, doi:10.1029/2004GL019491.

Shapiro, N. M., M. Campillo, L. Stehly, and M. H. Ritzwoller (2005), High-resolution surface-wave tomography from ambient seismic noise, *Science*, *307*(5715), 1615–1618.

Shapiro, N. M., M. H. Ritzwoller, and G. D. Bensen (2006), Source location of the 26 sec microseism from cross-correlations of ambient seismic noise, *Geophys. Res. Lett.*, *33*, L18310, doi:10.1029/2006GL027010.

Snieder, R. (2004), Extracting the Green's function from the correlation of coda waves: A derivation based on stationary phase, *Phys. Rev. E*, *69*(4), 046610, doi:10.1103/PhysRevE.69.046610.

Stachnik, J. C., A. F. Sheehan, D. W. Zietlow, Z. Yang, J. Collins, and A. Ferris (2012), Determination of New Zealand ocean bottom seismometer orientation via Rayleigh-wave polarization, *Seismol. Res. Lett.*, *83*(4), 704–713, doi:10.1785/0220110128.

van Wijk, K., T. D. Mikesell, V. Schulte-Pelkum, and J. Stachnik (2011), Estimating the Rayleigh-wave impulse response between seismic stations with the cross terms of the Green tensor, *Geophys. Res. Lett.*, *38*, L16301, doi:10.1029/2011GL047442.

Webb, S. C. (1998), Broadband seismology and noise under the ocean, *Rev. Geophys.*, *36*(1), 1–38, doi:10.1029/97RG02287.

Yang, Y., and M. H. Ritzwoller (2008), Characteristics of ambient seismic noise as a source for surface wave tomography, *Geochem. Geophys. Geosyst.*, *9*(2), Q02008, doi:10.1029/2007GC001814.